Published online: 2019-09-02

Original Article

Anatomical Variations of the Temporomesial Structures in Normal Adult Brain - A Cadaveric Study

Suresh Kumar Parmar, Nupur Pruthi[1], Roopa Ravindranath, Yogitha Ravindranath, Sampath Somanna[1], Mariamma Philip[2]

Department of Anatomy, St. John's Medical College, Departments of [1]Neurosurgery and [2]Biostatistics, National Institute of Mental Health and Neurosciences, Bengaluru, Karnataka, India

Abstract

Background: Despite significant evolutional, functional, and clinical interest, the anatomical variations of the temporomesial structures in cadaveric samples have received little attention. This study was undertaken to document the anatomical variations observed in the temporal lobe of human brain with emphasis on the structures present in temporomesial region. **Materials and Methods:** Using 26 postmortem cadaveric cerebral hemispheres (13 right and 13 left hemispheres), several neurosurgically significant mesial structures were studied by blunt dissection under the operating microscope. The observed surface-based qualitative variations and right-left asymmetries were tabulated under well-defined, moderately defined, and ill-defined classification. **Results:** Among the areas, uncus (100%), limen insulae (88.4%), rhinal sulcus and hippocampus (81%), intralimbic gyrus (77%), Heschl's gyrus (73%), gyrus ambiens, semilunar gyrus, sulcus semiannularis, and calcar avis (69.2%) were well defined, and band of Giacomini (38.4%) was found to be distinctly ill-defined areas in the list. Further, our analysis confirmed the presence of consistent left-greater-than-right asymmetry in all the areas of interest in temporal region under well-defined category. Rightward asymmetry was noticed in moderately defined and ill-defined classification. However, no asymmetry was detected in the uncal region. *P* value for all the obtained results was >0.05. **Conclusion:** Our study offers a preliminary anatomic foundation toward the better understanding of temporal lobe structures. These variations may prove valuable to neurosurgeons when designing the appropriate and least traumatic surgical approaches in operating the temporomesial lesions.

Keywords: *Amygdala, anatomy, asymmetry, epilepsy, Heschl's gyrus, hippocampus limen insulae*

Introduction

The anatomy of the human temporal lobe is complex, to say the least. It is one of the common locations for several brain pathologies such as gliomas, vascular malformations, mesial temporal scleroses, and viral infections. It is responsible for auditory perception,[1] memory,[2] speech,[3] language comprehension,[4] emotional responses,[5] visual perception,[6] and facial recognition[7] among various known functions.

Several reports have been published on the neurosurgical anatomy of the medial temporal structures.[8-12] However, a detailed cadaveric account of the anatomical variability and symmetrical pattern of the medial temporal structures, namely uncus, Heschl's gyrus, limen insulae, dentate gyrus, fasciolar gyrus, intralimbic gyrus, band of Giacomini, uncinate gyrus, gyrus ambiens, sulcus semiannularis, semilunar gyrus, rhinal sulcus, amygdale, and hippocampus is still lacking.

Therefore, the purpose of this macroscopic cadaveric study was to address the anatomical alterations, among

Access this article online

Quick Response Code:

Website: www.ruralneuropractice.com

DOI: 10.4103/jnrp.jnrp_73_18

Address for correspondence: Dr. Nupur Pruthi, Department of Neurosurgery, National Institute of Mental Health and Neurosciences, Bengaluru - 560 029, Karnataka, India. E-mail: pruthi_nupur@yahoo.co.in

This is an open access journal, and articles are distributed under the terms of the Creative Commons Attribution-NonCommercial-ShareAlike 4.0 License, which allows others to remix, tweak, and build upon the work non-commercially, as long as appropriate credit is given and the new creations are licensed under the identical terms.

For reprints contact: reprints@medknow.com

How to cite this article: Parmar SK, Pruthi N, Ravindranath R, Ravindranath Y, Somanna S, Philip M. Anatomical variations of the temporomesial structures in normal adult brain - A cadaveric study. J Neurosci Rural Pract 2018;9:317-25.

the aforementioned areas. Normal variations in these structures need to be well defined before one can use these structures to describe abnormal conditions. Further, correlating this topographical anatomical knowledge with existing radiological and surgical approaches may help to plan the most apt and safest surgical interventions.

Anatomical consideration

The temporal lobe lies inferior to the lateral sulcus (sylvian fissure) and imaginary horizontal line (temporooccipital line), limited posteriorly by an another imaginary vertical line (lateral parietotemporal line) joining the preoccipital notch to the parietooccipital sulcus [Figure 1].[13]

The temporal lobe has four surfaces: (1) the basal surface, (2) the lateral surface, (3) the superior or opercular surface, and (4) the mesial surface. The superior surface is limited posteriorly by the Heschl's gyrus, the most anterior of the transverse temporal gyri, which blends around the margin of the sylvian fissure into the superior temporal gyrus.[14] Owing to the complexity, mediobasal temporal lobe was divided into three regions in an anteroposterior plane: the anterior segment extending from the rhinal sulcus to the choroidal point; the middle segment extending from the choroidal point to the posterior aspect of the quadrigeminal plate; and the posterior segment consisting of the mediobasal temporal lobe posterior to the quadrigeminal plate.[10,11,15]

The anterior segment of mesial surface of temporal region is formed by the uncus and the entorhinal cortex. The uncus has an anterior and a posterior segment, which come together at a medially directed prominence, the apex of the uncus. The anterior segment of the uncus, a part of parahippocampal gyrus, encloses the semilunar gyrus and the ambient gyrus. The semilunar gyrus is positioned on the upper part of the anterior segment, above the cortical nucleus of amygdala. Superolaterally, this gyrus is isolated from the anterior perforated substance by the entorhinal sulcus and optic tract and anteromedially, from the ambient gyrus by the semiannular sulcus. The ambient gyrus, formed mainly by the entorhinal cortex, occupies the anterior and inferior parts of this segment. Superior and inferior division of the posterior uncal segment are separated by uncal sulcus. The inferior part, formed by the parahippocampal gyrus, is occupied by the entorhinal area. Inferior surface of the anterior uncal segment is occupied by the entorhinal cortex which is limited on the lateral side by the rhinal sulcus anteriorly and the collateral sulcus posteriorly. The posterior limits of the entorhinal area and uncus are considered same. The hippocampal head forms the superior part of the uncus while fimbria of fornix is present at its posterior limit. Further, the superior part of uncus accommodates three small gyri, the uncinate gyrus, the band of Giacomini, and the intralimbic gyrus. The band of Giacomini is the continuation of the dentate gyrus. The intralimbic gyrus contains the CA3 and the CA4 regions of the hippocampal formation. Hippocampal tail is formed by the fasciolar gyrus and its continuation, the subsplenial gyrus located beneath the splenium [Figures 2-5].[10,11]

Figure 1: Superolateral surface of cerebrum showing temporal lobe demarcation. 1: Parietooccipital sulcus, 2: Preoccipital notch, 3: Lateral parietotemporal line, 4: Temporooccipital line

Materials and Methods

Donors under 60 years of age, without the history of neuropathological diseases in their clinical records, were included in the study. Twenty-six formalin-fixed human cerebral hemispheres (13 right and 13 left hemispheres) were obtained from human cadavers donated to the human brain tissue repository, Department of Neuropathology, NIMHANS, Bengaluru, India with informed consent of the relatives for use of the whole brain for biomedical research and education.

Dissection technique

Before dissection, the specimen-specific surface anatomy of the cerebral hemisphere was studied to direct the initial steps of the dissection. Dissection of the specimen was performed using wooden spatulas, blunt and fine forceps, and microdissectors with 1–3 mm tips. Lateral to medial sequential dissection, steps were undertaken using a binocular surgical dissection microscope under 6X to 40X magnification (Leica F12, Germany) and an indigenous surgical suction system. Numerous digital photographs were taken in different views of the specimen at every dissection step by a digital camera (NIKON D5200) with F-36, ISO-100 settings, and macrolens (Tamron SP AF 90 mm, f/2.8 Di macrolens) with wireless remote Speedlight (Nikon

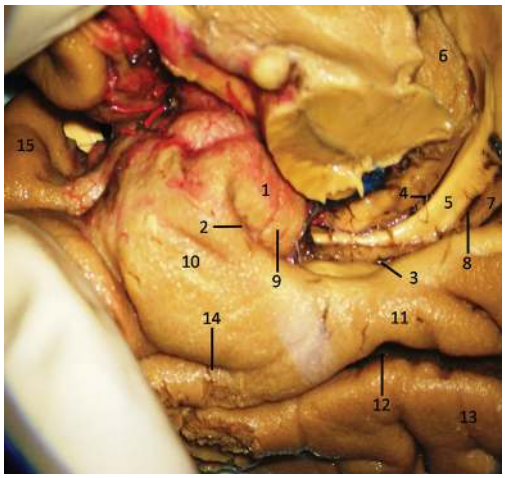

Figure 2: Medial Surface of Temporal lobe (anterior part) showing well-defined temporomesial structures: 1: Uncus, 2: Uncal notch, 3: Hippocampal sulcus, 4: Choroidal fissure; (between fornix and thalamus), 5: Fornix, 6: Pulvinar Thalamus, 7: Dentate gyrus, 8: Fimbrodentate sulcus, 9: Band of Giacomini, 10: Entorhinal cortex, 11: Parahippocampal gyrus, 12: Collateral sulcus, 13: Fusiform gyrus, 14: Rhinal sulcus, 15: Planum polare. Note: Region of interest are highlighted in bold

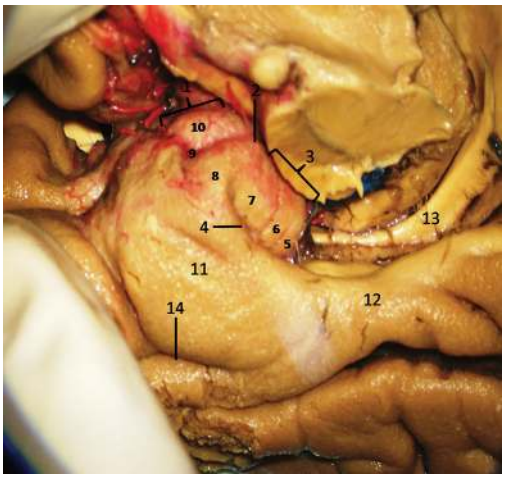

Figure 3: Medial Surface of Temporal lobe (anterior part) showing well-defined temporomesial structures: 1: Uncus anterior segment, 2: Uncal apex, 3: Uncus posterior segment, 4: Uncal notch, 5: Intralimbic gyrus, 6: Band of Giacomini, 7: Uncinate gyrus, 8: Gyrus ambiens, 9: Sulcus semiannularis, 10: Semilunar gyrus, 11: Entorhinal cortex, 12: Parahippocampal gyrus, 13: Fornix, 14: Rhinal sulcus. Note: Region of interest are highlighted in bold

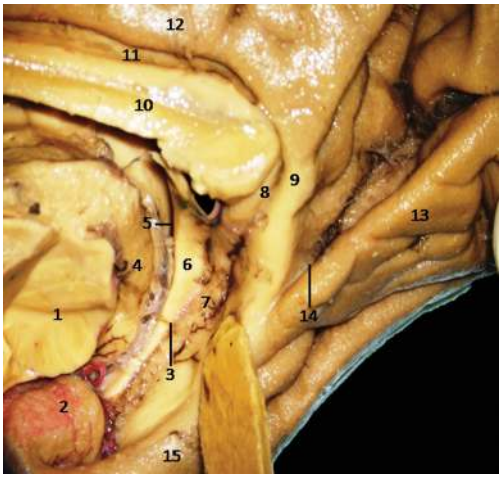

Figure 4: Medial Surface of Temporal lobe showing well-defined temporomesial structures: • 1: Midbrain (cut), 2: Uncus, 3: Fimbrodentate sulcus, 4: Pulvinar Thalamus, 5: Choroidal fissure (between fornix and thalamus), 6: Fornix, 7: Dentate gyrus, 8: Fasciolar gyrus, 9: Isthmus, 10: Corpus callosum, 11: Indusium griseum, 12: Cingulate gyrus, 13: Lingual gyrus, 14: Calcarine sulcus, 15: Parahippocampal gyrus. Note: Region of interest are highlighted in bold

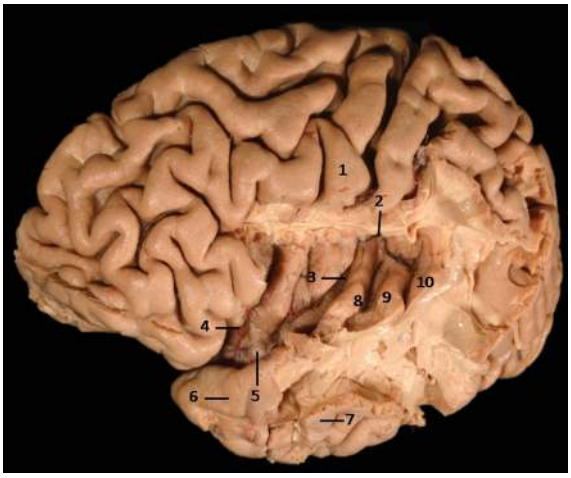

Figure 5: Lateral Surface of Temporal lobe with exposed insula showing well-defined limen insulae and Heschl's gyrus: 1: Central sulcus, 2: Superior limiting sulcus of insula, 3: Central sulcus of the insula, 4: Anterior limiting sulcus of insula, 5: Limen insulae, 6: Superior temporal gyrus, 7: Middle temporal gyrus, 8: Heschl's gyrus (Anterior transverse temporal gyrus), 9: Middle transverse temporal gyrus, 10: Posterior transverse temporal gyrus. Note: Region of interest are highlighted in bold

SB-R200) and the microscope camera (×6 magnification) for analysis and record. Between each dissection session, the specimens were kept in water to prevent dryness, to retain elasticity, and to facilitate a smoother dissection.

Surface-based qualitative analysis

After thorough identification of various dissected and undissected neuroanatomical areas on mesial temporal lobe in each cerebral hemisphere, different areas and its variations were qualitatively tabulated under well-defined, moderately defined, and ill-defined classification. Observed neuroanatomical areas having clearly distinguishable limits, boundaries, or features were identified as well defined, areas appearing vague, not having a clear description or limits as ill defined, and those with certain clarity in their presentation and distinguishable features falling neither of above two categories were classified as moderately defined areas.

Results

Among the twenty-six specimens, uncus (100%), limen insulae (88.4%), rhinal sulcus and hippocampus (81%), intralimbic gyrus (77%), Heschl's gyrus (73%), gyrus ambiens, semilunar gyrus, and sulcus semiannularis (69.2%) were found to be well defined,

and band of Giacomini (38.4%) was observed to be distinctly ill-defined areas in the list. Detailed anatomic identification of mesial temporal lobe areas under well-defined [Figures 2-8], moderately defined, and ill-defined [Figures 9 and 10] classification are summarized in Table 1.

Right and left asymmetry

Except in uncus, right and left asymmetry under well-defined, moderately defined, and ill-defined classification was noticed in all the observed neuroanatomical areas. Detailed symmetrical variations of both sides of different areas are summarized in Figure 11a-c and Table 2.

Chi-square test is based on the assumption that the expected count is >5 in 80% of the cells. This assumption is violated in our study in almost all parameters due to small number of cases reported under ill-defined and moderately defined category; hence, moderately defined and well-defined categories were combined and analyzed using Fisher's exact test which is used for 2 × 2 tables and is applied for small sample sizes.

Data were analyzed using Fisher's exact test. Interesting trends of consistent L > R asymmetry was observed in many areas, but these findings were statistically nonsignificant ($P > 0.05$). For areas limen insulae, dentate gyrus, fasciolar gyrus, intralimbic gyrus, band of Giacomini and hippocampus, P value was found to be 1.000. While P value for Heschl's gyrus ($P = 0.096$), uncinate gyrus ($P = 0.220$), gyrus ambiens ($P = 0.593$), sulcus semiannularis, semilunar gyrus, rhinal sulcus ($P = 0.593$) and amygdala ($P = 0.322$) were reported.

Discussion

As Sir William Osler aptly quoted, "variability is the law of life, and as no two faces are the same, so no two bodies are alike and no two individuals react alike and behave alike under the abnormal conditions which we know as disease." Learning of anatomy is incomplete without the knowledge of variations. It is an uncomfortable fact that unusual, sometimes wonderful, and often problematic anatomical variations occur in humans all the time, and neuroanatomy is no exception to this dogma. Medial temporal region is an extremely complex area of brain from both anatomical and surgical viewpoints. This area is a common site for various pathologies such as tumors.[16-18] It is also the most common region implied in drug-resistant epilepsy,[19] thereby serving as an area critical for various surgical approaches. Treatment of temporal lobe pathologies is demanding due to their close spatioanatomical relationship with important neurovascular structures such as optic radiations and internal carotid artery along with its branches. In parallel with developing microneurosurgical techniques, many new surgical approaches and anatomic corridors to this region have been described.[11,20-24] For a safe surgical approach, a neurosurgeon should be laced with sufficient anatomical knowledge of medial temporal lobe and possible variations in the neuroanatomical areas found in the temporal lobe region.[21] Although many studies have identified gyral morphology and their right-left asymmetries,[25,26] anatomic variations of mesial temporal lobe structures and their differences between the right and left hemispheres in the human brain *per se* were never reported.[27-30]

Temporal lobe asymmetry

Functional and structural asymmetries are the norms of human cerebral hemispheres. The renowned Broca's area for left hemispheric language specialization is a classical case of functional asymmetry.[31] Almost a century later, discovery of structural asymmetry between the right and left plana temporale[32] wherein the left side was found to be involved with the language function advocates the presence of some sort of interrelationship between the structural asymmetries and the lateralization of brain functions.

Uncus

Uncus was well defined in 100% of specimens with good interhemispheric symmetry. This could be due to the presence of well-developed underlying white fiber tracts.[33,34] These findings indicate that the area of uncus is quite consistent, both between hemispheres and across the specimens.[35] [Figures 2, 4, 9, 10, 11a-c and Tables 1, 2]. To the best of our knowledge, this is the first surface-based qualitative study of uncus reporting bilateral symmetry. However, in another postmortem study of schizophrenic temporal lobe, the uncus demonstrated R > L asymmetry.[35]

Heschl's gyrus

Heschl's gyrus was found to be well defined in 73% and moderately defined in 11.5% specimens [Figures 5, 12, 11a-c and Tables 1, 2]. This well-seen macroanatomical observation could be again due to the presence of underlying prominent white matter tracts.[33,34] Out of thirteen left-sided hemispheres, all (100%) specimens showed well-defined gyri. On the other hand, in 13 right-sided hemispheres studied, 6 (46%) right-sided hemispheres showed well-defined and 3 (23%) showed moderately defined and 4 (31%) reflected ill-defined gyri. This leftward asymmetrical distribution of Heschl's gyrus is in concurrence with various other studies reporting left-sided predominance of Heschl's gyrus which may be due to the known left hemisphere speech

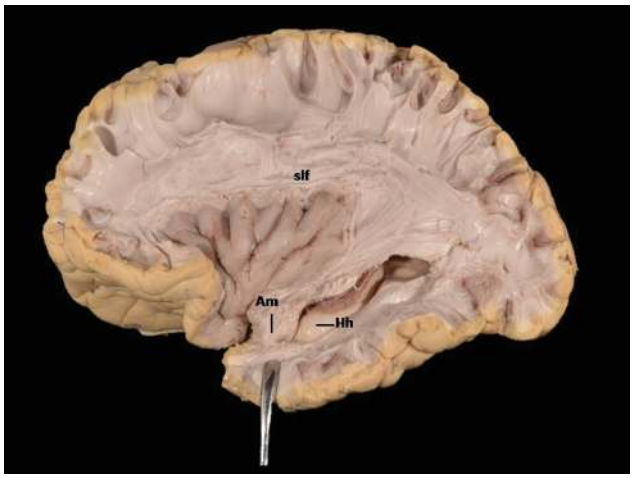

Figure 6: Lateral Surface of Temporal lobe (anterior part) showing ill-defined. Am-Amygdala (exposed) and well-defined Hh-Hippocampus (unexposed) Slf-Superior longitudinal fasciculus; of-Occipitofrontal fasciculus; icpl-Internal capsule-posterior limb. Note: Region of interest are highlighted in bold

Figure 7: Lateral Surface of Temporal lobe showing well-defined Hippocampus and other temporomesial structures. *Amygdala is removed in this specimen. 1: Hippocampus head, 2: Hippocampus body, 3: Hippocampus tail, 4: Anterior Choroidal point, 5: Fimbria, 6: Choroid plexus, 7: Collatral trigone, 8: Calcar avis, 9: Inferior horn of Lateral Ventricle. Note: Region of interest are highlighted in bold

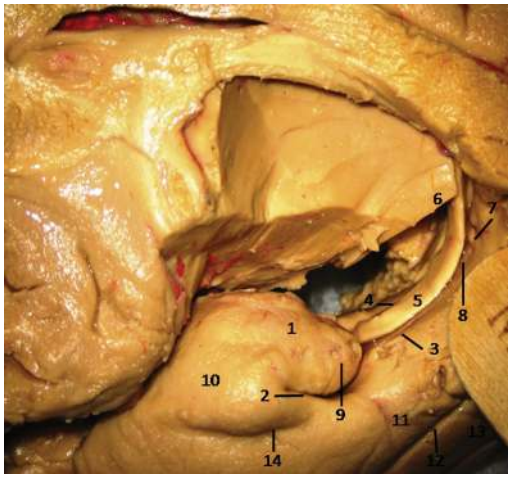

Figure 8: Medial Surface of Temporal lobe (anterior part) showing ill-defined temporomesial structures except uncus: 1: Uncus, 2: Uncal notch, 3: Hippocampal sulcus, 4: Choroidal fissure; (between fornix and thalamus), 5: Fornix, 6: Pulvinar Thalamus, 7: Dentate gyrus, 8: Fimbrodentate sulcus, 9: Band of Giacomini, 10: Entorhinal cortex, 11: Parahippocampal gyrus, 12: Collateral sulcus, 13: Fusiform gyrus, 14: Rhinal sulcus. Note: Region of interest are highlighted in bold

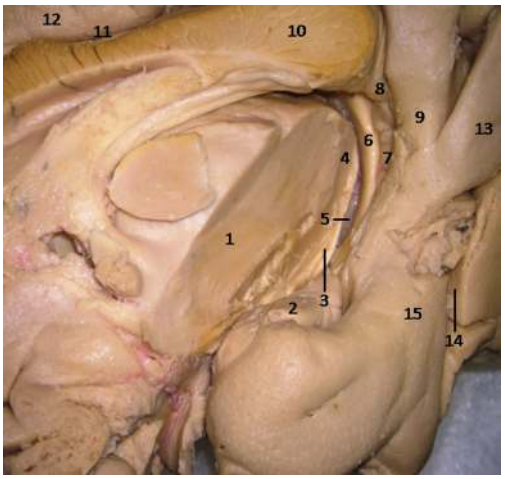

Figure 9: Medial Surface of Temporal lobe showing ill-defined temporomesial structures: 1: Thlamus (cut), 2: Uncus, 3: Fimbrodentate sulcus, 4: Pulvinar Thalamus, 5: Choroidal fissure (between fornix and thalamus), 6: Fornix, 7: Dentate gyrus, 8: Fasciolar gyrus, 9: Isthmus, 10: Corpus callosum, 11: Indusium griseum, 12: Cingulate gyrus, 13: Lingual gyrus, 14: Calcarine sulcus, 15: Parahippocampal gyrus. Note: Region of interest are highlighted in bold

dominance.[26,33,36-40] While certain postmortem studies have also reported rightward asymmetries in Heschl's gyrus.[32,41] However, there are few studies, reporting presence of bilateral symmetry in the surface area of the anterior Heschl's gyri[37] or in the area of primary auditory cortex.[42]

Limen insulae

The limen insulae is positioned in the bottom of the Sylvian fissure and forms the anterobasal portion of the insula [Figure 5]. Cytoarchitecturally, limen insulae consist of agranular and rostral dysgranular regions, which has connections with the primary olfactory cortex, amygdala, hippocampus, temporopolar cortex, and Brodmann area along with other perilimbic areas.[43,44] In view of these reports, we noticed strong morphological-positive correlation between limen insulae (well defined in 88.4%), hippocampus (well defined in 81%), and amygdale (well defined in 69.2%) [Figure 12 and Table 1]. In addition, all the 3 areas have shown leftward asymmetry, i.e., limen insulae – right: 77%; left: 100%, hippocampus – right: 77%; left: 85% and amygdale – right: 46%; left: 92.3% [Figure 11a-c and Table 2], yet again hinting to be a possible anatomical correlate of the lateralization of their functions.

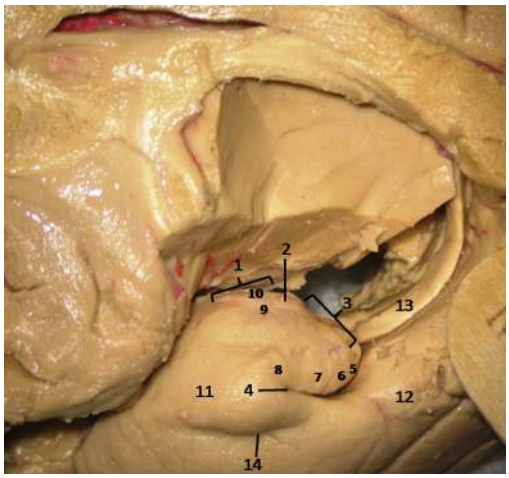

Figure 10: Medial Surface of Temporal lobe (anterior part) showing ill-defined temporomesial structures: 1: Uncus anterior segment, 2: Uncal apex, 3: Uncus posterior segment, 4: Uncal notch, 5: Intralimbic gyrus, 6: Band of Giacomini, 7: Uncinate gyrus, 8: Gyrus ambiens, 9: Sulcus semiannularis, 10: Semilunar gyrus, 11: Entorhinal cortex, 12: Parahippocampal gyrus, 13: Fornix, 14: Rhinal sulcus. Note: Region of interest are highlighted in bold

Table 1: Variability in various temporal lobe structures under well-defined, moderately defined, and ill-defined classification (*n*=26)

Areas	Well-defined, *n* (%)	Moderately defined, *n* (%)	Ill-defined, *n* (%)
Uncus	26 (100)	0	0
Heschl's gyrus	19 (73)	3 (11.5)	4 (15.3)
Limen insulae	23 (88.4)	2 (8)	1 (4)
Dentate gyrus	17 (65.3)	5 (19.2)	4 (15.3)
Fasciolar gyrus	17 (65.3)	5 (19.2)	4 (15.3)
Intralimbic gyrus	20 (77)	4 (15.3)	2 (8)
Band of Giacomini	10 (38.4)	6 (23)	10 (38.4)
Uncinate gyrus	21 (81)	4 (15.3)	1 (4)
Gyrus ambiens	18 (69.2)	4 (15.3)	4 (15.3)
Sulcus semiannularis	18 (69.2)	5 (19.2)	3 (11.5)
Semilunar gyrus	18 (69.2)	4 (15.3)	4 (15.3)
Rhinal sulcus	21 (81)	2 (8)	3 (11.5)
Amygdala	18 (69.2)	3 (11.5)	5 (19.2)
Hippocampus	21 (81)	4 (15.3)	1 (4)

n: Number of samples

Other areas of interest

Semilunar gyrus and gyrus ambiens separated by semilunar sulcus (sulcus semilunaris) overlying the amygdale form the anterior segment of uncus. In our study, we noticed cortical covering formed by the abovementioned sulcus and gyri showed surface relationship with the deeply located amygdale, i.e., semilunar gyrus was observed to be well defined in 69.2% and ill defined in 15.3%, gyrus ambiens was well defined in 69.2% and ill defined in 15.3%, and semilunar sulcus was well defined in 69.2% and ill defined in 11.5% of the total specimens studied, whereas amygdale was found to be well defined in 69.2% and ill defined in 19.2% of total samples studied. Thus, anterior uncal segment surface anatomy relationship of semilunar gyrus, gyrus ambiens, and semilunar sulcus was found to be proportional with deeply located amygdala. Similarly, the posterior uncal segment structures such as intralimbic gyrus (well defined 77%, ill defined in 8%) and uncinate gyrus (well defined in 81%, ill defined in 4%) showed proportional relationship with deeply located head of hippocampus (well defined in 81%, ill defined in 1%). However, band of Gioacomani, another area seen among posterior uncal segment, was found to be equally well defined and ill defined in 38.4% cases reflecting no definite proportional relationship with deeply located hippocampal head containing dentate gyrus [Figures 2-4, 7-12 and Tables 1, 2].

Band of Giacomini

Most of the dentate gyrus is not exposed onto the brain surface; its visible parts in medial surface of sagittal half of cerebrum include the band of Giacomini in the posterior uncal segment, the margo denticulatus in the head, and fasciolar gyrus in the tail of hippocampus.[45] Similar to the findings of earlier studies,[45] the present study concurred with the band of Giacomini which was found to be not the most visible part of dentate gyrus; it was well defined only in 38.4% of specimens in our observation. On the other hand, in comparison to the band of Giacomini, the margo denticulatus part of dentate gyrus and fasciolar gyrus was well defined in 65.3% of cases.

Intralimbic and uncinate gyri form the cortical covering of hippocampal head. In our study, we found a positive correlation between the surface anatomical (intralimbic gyrus well defined in 77% and uncinate gyrus well defined in 81% cases) and subcortical structures (hippocampal head well defined in 81% cases).

The rhinal sulcus courses along the entire length of amygdala, head of the and body (mid half) of hippocampus, thereby stretching across the entire length of uncus.[46] In the present study, a strong positive correlation was found between the rhinal sulcus and posterior uncal segment. Rhinal sulcus was well defined in 81% of samples with a strong positive correlation with corresponding posterior uncal segment showing intralimbic gyrus in 77% and uncinate gyri in 81% samples. On the other hand, the band of Giacomini (38.4%), one of the parts of posterior uncal segments, showed negative correlation with rhinal sulcus (81%). A near-positive correlation was observed among anterior uncal segment consisting of semilunar and ambiens gyri (69.2%) and semilunar sulcus (69.2%) with rhinal sulcus (81%). Similarly, uncinate gyrus (81%) showed strong positive correlation

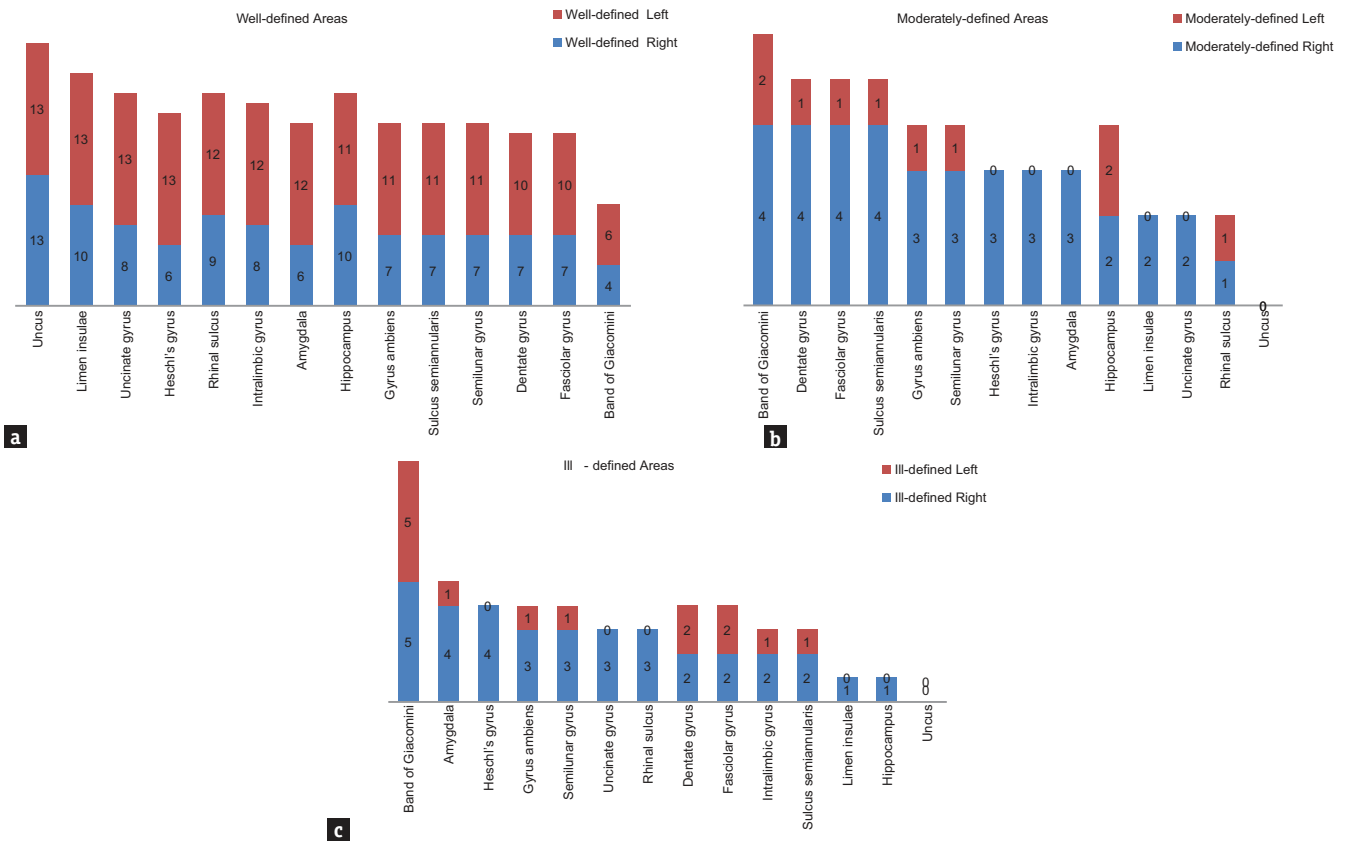

Figure 11: Bar graph showing the variability under well-defined, moderately defined, and ill-defined classification of temporal lobe structures (*n* = 26)

Table 2: Asymmetrical pattern in temporal lobe structures under well-defined, moderately defined, and ill-defined classification (*n*=26)

Neuroanatomical areas	Well-defined, *n* (%)		Moderately defined, *n* (%)		Ill-defined, *n* (%)	
	Right side	Left side	Right side	Left side	Right side	Left side
Uncus	13 (100)	13 (100)	-	-	-	-
Heschl's gyrus	6 (46)	13 (100)	3 (23)	-	4 (31)	-
Limen insulae	10 (77)	13 (100)	2 (15.3)	-	1 (8)	-
Dentate gyrus	7 (54)	10 (77)	4 (31)	1 (8)	2 (15.3)	2 (15.3)
Fasciolar gyrus	7 (54)	10 (77)	4 (31)	1 (8)	2 (15.3)	2 (15.3)
Intralimbic gyrus	8 (61.5)	12 (92.3)	3 (23)	-	2 (15.3)	1 (8)
Band of Giacomini	4 (31)	6 (46)	4 (31)	2 (15.3)	5 (38.4)	5 (38.4)
Uncinate gyrus	8 (61.5)	13 (100)	2 (15.3)	-	3 (23)	-
Gyrus ambiens	7 (54)	11 (85)	3 (23)	1 (8)	3 (23)	1 (8)
Sulcus semiannularis	7 (54)	11 (85)	4 (31)	1 (8)	2 (15.3)	1 (8)
Semilunar gyrus	7 (54)	11 (85)	3 (23)	1 (8)	3 (23)	1 (8)
Rhinal sulcus	9 (69.2)	12 (92.3)	1 (8)	1 (8)	3 (23)	-
Amygdala	6 (46)	12 (92.3)	3 (23)	-	4 (31)	1 (8)
Hippocampus	10 (77)	11 (85)	2 (15.3)	2 (15.3)	1 (8)	-

n: Number of samples

with hippocampal head (81%) [Figures 2-4, 7-12 and Tables 1, 2].

The most striking result of the present study was the consistent L > R asymmetry in most of the areas, except uncus which showed bilateral symmetrical pattern. Leftward asymmetry was observed in all the areas under well-defined category. On the contrary, rightward asymmetry was noticed under moderately defined and ill-defined categories but with lower percentage values, thereby reflecting overall leftward asymmetry in temporal lobe areas [Table 2]. Our findings were in concurrence with various other studies.[33,36,42] Rightward

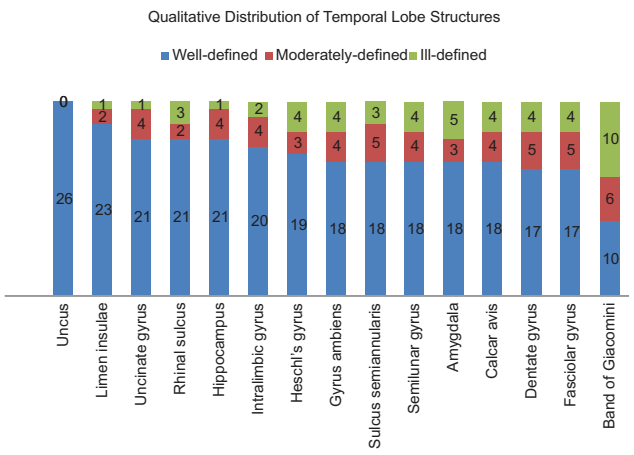

Figure 12: Bar graphs showing the extent of right-left asymmetry and variability in well-defined, moderately defined, and ill-defined structures in temporal lobe. Numerical indicates the right-left variability among the samples ($n = 26$)

symmetry observations were reported by other studies in Heschl's gyrus[47] and primary auditory cortex.[39] The present study is of its kind as it involves exploration of temporomesial region through the blunt dissection technique. The reported variations are not only difficult to visualize with routinely used 3 Tesla magnetic resonance imaging but also equally challenging to reproduce the similar observations owing to low resolution. On the other hand, the blunt dissection technique is inexpensive; more educative skill with high reproducibility and its incorporation into neurosurgical education becomes need of the hour.

Limitations

- Small sample size
- Gender-specific and handedness analysis and observation.

Conclusion

Temporal lobe seems to be a seat of neuroevolutionary engineering reflecting the makeup of all types of cortices ranging from small poorly developed 3-layered archicortex (hippocampus, dentate, and fasciolar gyri) to 3–4-layered transitional region (entorhinal cortex) to a well-developed 6-layered neocortex (Heschl's gyrus). It will not be equally surprising to find anatomical variations in this highly transitional region, especially in medial temporal lobe. Mesial temporal lobe being the area of high neurosurgical significance, the information generated from our surface-based qualitative observations may yield further insight into the neurosurgical anatomy and may contribute to the development of safe and minimally invasive neurosurgical procedures for neurosurgeons.

The consistent finding of L > R asymmetry in the present study further substantiates the prevalent notion that the left temporal lobe is slightly larger than the right, and this could be attributed to the volume of white matter which may be due to the disparity in the cellular arrangement of the two hemispheres. These findings also raise an interesting question whether "bigger is better" or these structural asymmetries found in mesial temporal lobe structures are in turn may be related to some sort of abnormal functional organization in waiting.

Acknowledgement

The authors wish to thank Human Brain Bank, Department of Neuropathology, NIMHANS, Bangalore for providing formalin fixed brain specimens for the present study and Ramaiah Advanced Learning Centre, Ramaiah Institute of Neurosciences and Department of Anatomy, Ramaiah Medical College, Bangalore for specimens preparation.

Financial support and sponsorship

Nil.

Conflicts of interest

There are no conflicts of interest.

References

1. Kimura D. Some effects of temporal-lobe damage on auditory perception. Can J Psychol 1961;15:156-65.
2. Dolcos F, LaBar KS, Cabeza R. Interaction between the amygdala and the medial temporal lobe memory system predicts better memory for emotional events. Neuron 2004;42:855-63.
3. Binder JR, Frost JA, Hammeke TA, Bellgowan PS, Springer JA, Kaufman JN, *et al.* Human temporal lobe activation by speech and nonspeech sounds. Cereb Corte×2000;10:512-28.
4. Kutas M, Federmeier KD. Electrophysiology reveals semantic memory use in language comprehension. Trends Cogn Sci 2000;4:463-70.
5. Gloor P, Olivier A, Quesney LF, Andermann F, Horowitz S. The role of the limbic system in experiential phenomena of temporal lobe epilepsy. Ann Neurol 1982;12:129-44.
6. Murray EA, Bussey TJ, Saksida LM. Visual perception and memory: A new view of medial temporal lobe function in primates and rodents. Annu Rev Neurosci 2007;30:99-122.
7. Milner B. Visual recognition and recall after right temporal-lobe excision in man. Neuropsychologia 1968;6:191-9.
8. Huther G, Dörfl J, Van der Loos H, Jeanmonod D. Microanatomic and vascular aspects of the temporomesial region. Neurosurgery 1998;43:1118-36.
9. Wen HT, Rhoton AL Jr., de Oliveira E, Cardoso AC, Tedeschi H, Baccanelli M, *et al.* Microsurgical anatomy of the temporal lobe: Part 1: Mesial temporal lobe anatomy and its vascular relationships as applied to amygdalohippocampectomy. Neurosurgery 1999;45:549-91.
10. Fernández-Miranda JC, de Oliveira E, Rubino PA, Wen HT, Rhoton AL Jr. Microvascular anatomy of the medial temporal region: Part 1: Its application to arteriovenous malformation surgery. Neurosurgery 2010;67:237-76.
11. Kucukyuruk B, Richardson RM, Wen HT, Fernandez-Miranda JC, Rhoton AL Jr. Microsurgical anatomy of the temporal lobe and its implications on temporal lobe epilepsy surgery. Epilepsy Res Treat 2012;2012:769825.

12. Renella RR, editor. Surgery of the temporo-medial region. In: Microsurgery of the Temporo-Medial Region. 1st ed. Vienna: Springer Science & Business Media; 2012. p. 122-57.
13. Standring S, editor. Cerebral hemispheres. In: Gray's Anatomy: The Anatomical Basis of Clinical Practice. 41st ed. London: Elsevier Health Sciences; 2015. p. 382-4.
14. Tanriover N, Rhoton AL Jr., Kawashima M, Ulm AJ, Yasuda A. Microsurgical anatomy of the insula and the sylvian fissure. J Neurosurg 2004;100:891-922.
15. Straus D, Byrne RW, Sani S, Serici A, Moftakhar R. Microsurgical anatomy of the transsylvian translimen insula approach to the mediobasal temporal lobe: Technical considerations and case illustration. Surg Neurol Int 2013;4:159.
16. Wolf HK, Campos MG, Zentner J, Hufnagel A, Schramm J, Elger CE, *et al.* Surgical pathology of temporal lobe epilepsy. Experience with 216 cases. J Neuropathol Exp Neurol 1993;52:499-506.
17. Larjavaara S, Mantyla R, Salminen T, Haapasalo H, Raitanen J, Jääskeläinen J, *et al.* Incidence of gliomas by anatomic location. Neuro Oncol 2007;9:319-25.
18. Tassi L, Meroni A, Deleo F, Villani F, Mai R, Russo GL, *et al.* Temporal lobe epilepsy: Neuropathological and clinical correlations in 243 surgically treated patients. Epileptic Disord 2009;11:281-92.
19. Asadi-Pooya AA, Stewart GR, Abrams DJ, Sharan A. Prevalence and incidence of drug-resistant mesial temporal lobe epilepsy in the United States. World Neurosurg 2017;99:662-6.
20. Voigt K, Yaşargil MG. Cerebral cavernous haemangiomas or cavernomas. Incidence, pathology, localization, diagnosis, clinical features and treatment. Review of the literature and report of an unusual case. Neurochirurgia (Stuttg) 1976;19:59-68.
21. Yaşargil MG, Cravens GF, Roth P. Surgical approaches to "inaccessible" brain tumors. Clin Neurosurg 1988;34:42-110.
22. Campero A, Tróccoli G, Martins C, Fernandez-Miranda JC, Yasuda A, Rhoton AL Jr., *et al.* 22 Microsurgical approaches to the medial temporal region: An anatomical study. Neurosurgery 2006;59:279-307.
23. Yaşargil MG, Krayenbühl N, Roth P, Hsu SP, Yaşargil DC. The selective amygdalohippocampectomy for intractable temporal limbic seizures. J Neurosurg 2010;112:168-85.
24. Türe U, Harput MV, Kaya AH, Baimedi P, Firat Z, Türe H, *et al.* The paramedian supracerebellar-transtentorial approach to the entire length of the mediobasal temporal region: An anatomical and clinical study. Laboratory investigation. J Neurosurg 2012;116:773-91.
25. Pfeifer RA. Myelogenetisch-Anatomische Untersuchungen Über Das Kortikale Ende Der Hörleitung. Leipzig: Teubner, BG; 1920.
26. Economo CV, Horn L. Uber Windungsrelief, mare und rindenarchitektonik der supratemporalfliiche, ihre individuellen und ihre seitenunterschiede. Z Gesamte Neurol Psychiatr 1930;130:678-57.
27. Ono M, Kubik SA. Atlas of the Cerebral Sulci. Stuttgart, New York, Thieme: Thieme Med. Publication; 1990.
28. Roper SN, Rhoton AL Jr. Surgical anatomy of the temporal lobe. Neurosurg Clin N Am 1993;4:223-31.
29. DeFelipe J, Fernández-Gil MA, Kastanauskaite A, Bote RP, Presmanes YG, Ruiz MT, *et al.* Macroanatomy and microanatomy of the temporal lobe. Semin Ultrasound CT MR 2007;28:404-15.
30. Kiernan JA. Anatomy of the temporal lobe. Epilepsy Res Treat 2012;2012:1-12.
31. Broca P. Perte de la parole. Ramollisement chronique et destruction partielle du lobe antérieur gauche du cerveau. Bull Soc Anthr 1861;2:235-8.
32. Geschwind N, Levitsky W. Human brain: Left-right asymmetries in temporal speech region. Science 1968;161:186-7.
33. Penhune VB, Zatorre RJ, MacDonald JD, Evans AC. Interhemispheric anatomical differences in human primary auditory cortex: Probabilistic mapping and volume measurement from magnetic resonance scans. Cereb Cortex 1996;6:661-72.
34. Anderson B, Southern BD, Powers RE. Anatomic asymmetries of the posterior superior temporal lobes: A postmortem study. Neuropsychiatry Neuropsychol Behav Neurol 1999;12:247-54.
35. Highley JR, Walker MA, Esiri MM, McDonald B, Harrison PJ, Crow TJ. Schizophrenia and the frontal lobes post-mortem stereological study of tissue volume.Br J Psychiatry 2001;178:337-43.
36. Rademacher J, Caviness VS Jr., Steinmetz H, Galaburda AM. Topographical variation of the human primary cortices: Implications for neuroimaging, brain mapping, and neurobiology. Cereb Cortex 1993;3:313-29.
37. Kulynych JJ, Vladar K, Jones DW, Weinberger DR. Gender differences in the normal lateralization of the supratemporal cortex: MRI surface-rendering morphometry of heschl's gyrus and the planum temporale. Cereb Cortex 1994;4:107-18.
38. Rademacher J, Morosan P, Schormann T, Schleicher A, Werner C, Freund HJ, *et al.* Probabilistic mapping and volume measurement of human primary auditory cortex. Neuroimage 2001;13:669-83.
39. Morosan P, Rademacher J, Schleicher A, Amunts K, Schormann T, Zilles K, *et al.* Human primary auditory cortex: Cytoarchitectonic subdivisions and mapping into a spatial reference system. Neuroimage 2001;13:684-701.
40. Penhune VB, Cismaru R, Dorsaint-Pierre R, Petitto LA, Zatorre RJ. The morphometry of auditory cortex in the congenitally deaf measured using MRI. Neuroimage 2003;20:1215-25.
41. Chi JG, Dooling EC, Gilles FH. Left-right asymmetries of the temporal speech areas of the human fetus. Arch Neurol 1977;34:346-8.
42. Galaburda A, Sanides F. Cytoarchitectonic organization of the human auditory cortex. J Comp Neurol 1980;190:597-610.
43. Mufson EJ, Mesulam MM. Insula of the old world monkey. II: Afferent cortical input and comments on the claustrum. J Comp Neurol 1982;212:23-37.
44. Mesulam MM, Mufson EJ. Insula of the old world monkey. III: Efferent cortical output and comments on function. J Comp Neurol 1982;212:38-52.
45. Duvernoy HM. Anatomy of the hippocampus. In: The Human Hippocampus. An Atlas of Applied Anatomy. Munich: J.F. Bergmann-Verlag; 1988. p. 31.
46. Huntgeburth SC, Petrides M. Morphological patterns of the collateral sulcus in the human brain. Eur J Neurosci 2012;35:1295-311.
47. Campain R, Minckler J. A note on the gross configurations of the human auditory cortex. Brain Lang 1976;3:318-23.